

# Residual block fully connected DCNN with categorical generalized focal dice loss and its application to Alzheimer's disease severity detection

Adi Alhudhaif<sup>Corresp., 1</sup>, Kemal Polat<sup>2</sup>

<sup>1</sup> Department of Computer Science, College of Computer Engineering and Sciences in Al-kharj, Prince Sattam Bin Abdulaziz University, Al-kharj, Saudi Arabia

<sup>2</sup> Department of Electrical and Electronics Engineering, Faculty of Engineering, Bolu Abant Izzet Baysal University, Bolu, TURKEY

Corresponding Author: Adi Alhudhaif  
Email address: a.alhudhaif@psau.edu.sa

**Background:** Alzheimer's disease (AD) is a disease that manifests itself with a deterioration in all mental activities, daily activities, and behaviors, especially memory, due to the constantly increasing damage to some parts of the brain as people age. Detecting AD at an early stage is a significant challenge. Various diagnostic devices are used to diagnose AD. MRI (Magnetic Resonance) devices are widely used to analyze and classify the stages of AD. However, the time-consuming process of recording the affected areas of the brain in the images obtained from these devices is another challenge. Therefore, conventional techniques cannot detect the early stage of AD.

**Methods:** This study proposes a deep learning model supported by a fusion loss model that includes fully connected layers and residual blocks to solve the above-mentioned challenges. The proposed model has been trained and tested on the publicly available T1-weighted MRI-based KAGGLE dataset. Data augmentation techniques were used after various preliminary operations were applied to the data set.

**Results:** The proposed model effectively classified four AD classes in the KAGGLE dataset. The proposed model reached the test accuracy of 0.973 in binary classification and 0.982 in multi-class classification thanks to experimental studies and provided a superior classification performance than other studies in the literature.

# 1 Residual Block Fully Connected DCNN with Categorical Generalized 2 Focal Dice Loss and its Application to Alzheimer's Disease Severity 3 Detection

4

5 Adi Alhudhaif<sup>1\*</sup> and Kemal Polat<sup>2</sup>

6

7 <sup>1</sup>Department of Computer Science, College of Computer Engineering and Sciences in Al-kharj,  
8 Prince Sattam bin Abdulaziz University, P.O. Box 151, Al-Kharj 11942, Saudi Arabia,  
9 e-mail: [A.alhudhaif@psau.edu.sa](mailto:A.alhudhaif@psau.edu.sa)

10

11 Department of Electrical and Electronics Engineering, Faculty of Engineering, Bolu Abant Izzet  
12 Baysal University, Bolu, Turkey  
13 e-mail: [kpolat@ibu.edu.tr](mailto:kpolat@ibu.edu.tr)

14

## 15 Corresponding Author:

16 Dr. Adi Alhudhaif

17 Department of Computer Science, College of Computer Engineering and Sciences in Al-kharj,  
18 Prince Sattam bin Abdulaziz University, P.O. Box 151, Al-Kharj 11942, Saudi Arabia19 Email address: [A.alhudhaif@psau.edu.sa](mailto:A.alhudhaif@psau.edu.sa)

20

## 21 Abstract

22

23 **Background:** Alzheimer's disease (AD) is a disease that manifests itself with a deterioration in  
24 all mental activities, daily activities, and behaviors, especially memory, due to the constantly  
25 increasing damage to some parts of the brain as people age. Detecting AD at an early stage is a  
26 significant challenge. Various diagnostic devices are used to diagnose AD. MRI (Magnetic  
27 Resonance) devices are widely used to analyze and classify the stages of AD. However, the time-  
28 consuming process of recording the affected areas of the brain in the images obtained from these  
29 devices is another challenge. Therefore, conventional techniques cannot detect the early stage of  
30 AD.31 **Methods:** This study proposes a deep learning model supported by a fusion loss model that  
32 includes fully connected layers and residual blocks to solve the above-mentioned challenges. The  
33 proposed model has been trained and tested on the publicly available T1-weighted MRI-based  
34 KAGGLE dataset. Data augmentation techniques were used after various preliminary operations  
35 were applied to the data set.

36

37 **Results:** The proposed model effectively classified four AD classes in the KAGGLE dataset. The  
38 proposed model reached the test accuracy of 0.973 in binary classification and 0.982 in multi-class  
39 classification thanks to experimental studies and provided a superior classification performance  
40 than other studies in the literature.

41

42 **Keywords:** Alzheimer's disease; Categorical Generalized Focal Dice Loss; Deep learning; New hybrid  
43 models; classification

44

## 45 **Introduction**

46

47 The brain is a vital organ that contains memory and manages thoughts and decision-making [Armstrong et  
48 al., 2009]. AD is one of the causes of dementia. In AD, beta-amyloid and phosphorylated tau proteins  
49 accumulate excessively, which causes brain cell degeneration [Alzheimer's disease facts and figures, 2022].

50 AD is an irreversible disease that causes progressive brain deterioration. Memory cells gradually die,  
51 causing an increasing shrinkage in the brain [Alberdi et al., 2018]. AD is a fatal neurological disease with  
52 a life expectancy of 4-8 years after diagnosis [Babalola et al., 2009 ]. This disease, which can be seen at  
53 any age, is more common in people over 65 [Coppola et al., 2013; Chandra et al., 2019].

54 - -

55 According to official figures in the United States, 121,499 people died from AD in 2019. AD was  
56 ranked sixth among the causes of death in 2019 when Covid-19 was among the top 10 reasons. In addition,  
57 In 2020 and 2021, it was shown as the seventh leading cause of death. Total payments made in 2022 for  
58 health care, long-term care, and hospice services for people aged 65 and over with dementia are estimated  
59 at \$321 billion [Alzheimer's disease facts and figures, 2022].

60 Several different computer-assisted neuroimaging methods can diagnose AD. In light of clinical experience,  
61 MRI has become almost standardized in these imaging modalities. Although AD is incurable, its  
62 progression can be slowed with early diagnosis and treatment [Gopinadhan et al., 2022].

63 In the last decades, many machine learning-based and specifically deep learning-based approaches to  
64 diagnosing AD have been presented. If we summarize the previous studies in the literature, classification  
65 based on segmentation of brain images was used for early diagnosis of AD by Mehmood et al. For the AD  
66 classification, the VGG network was used for transfer learning [Mehmood et al., 2021]. Lahmiri et al. used  
67 Deep Convolutional Neural Networks (DCNN) to increase the diagnostic sensitivity of AD. Besides, the  
68 KNN approach was used to filter the number of features [Lahmiri, 2023]. Shanmugam et al. analyzed the  
69 success of three pre-trained networks, GoogLeNet, AlexNet, and ResNet-18, in classifying AD's stages  
70 [Shanmugam et al., 2022]. Frizzell et al. conducted a systematic literature review covering studies  
71 conducted between 2009 and 2020 for the diagnosis of AI-based AD using the PubMed database. In the  
72 review, images consisting of 3 different classes, including normal aging, mild cognitive impairment, and  
73 AD, obtained from MRI, were examined, and comparatively analyzed with the proposed artificial  
74 intelligence algorithms [Frizzell et al., 2022]. Kumar et al. have proposed a classification model that uses  
75 the AlexNet framework to diagnose AD at an early stage from MR images [Kumar et al., 2022]. Jung et al.  
76 proposed a new conditional generative adversarial network (cGAN) capable of synthesizing high-quality

77 3D MR images. The proposed model consists of an attention-based 2D generator, a 2D parser, and a 3D  
78 splitter that can synthesize 2D slices from 3D MR images [Jung et al., 2023]. Liu et al. proposed the Monte  
79 Carlo Aggregated Neural Network model combining ResNet50 and Monte Carlo sampling for early AD  
80 detection. The proposed model is trained on 2D slices obtained from 3D MR images [Liu et al., 2023].  
81 Sharma et al. proposed an artificial neural network model using the VGG16 deep learning network as a  
82 feature extractor for the classification of 4 different stages of AD [Sharma et al., 2022]. Alorf et al. proposed  
83 a multi-label spoofing model using the Stacked Sparse Autoencoder and Brain Connectivity Graph  
84 Convolutional Network models for the six stages of AD obtained from the rs-fMR imaging device [Alorf  
85 et al., 2022]. Raghavaiah et al. trained a DCNN-based model on fMRI and MRI to diagnose AD from  
86 specific sound control information. It is fed to the proposed model via an image converter with decomposed  
87 parameters from fMRI and MRI [Ravagiah et al., 2021]. Loddo et al. proposed a deep learning model  
88 combining AlexNet, ResNet101, and Inception-ResNet-V2 for AD classification [Loddo et al., 2021].  
89 Studies in the literature achieved test success of up to 99% in ADNI and OASIS data sets with deep learning  
90 models. As far as we know in the literature, only Loddo et al. and Sharma et al. tested their models on the  
91 Kaggle dataset. The Kaggle dataset is a dataset that challenges models due to both its small size and  
92 difficulties in distinguishing between classes.

93

94 Manual classification of AD on brain images obtained from MRI devices is time-consuming. At the same  
95 time, AD is very similar to what happens in the brain with aging. Therefore, it is a challenging task to  
96 diagnose AD by clinicians. Thus, Deep learning-based computer-aided systems, which often achieve higher  
97 success than clinicians, gain more significant importance for AD classification.

98

99 **In summary, the main contributions of this paper to the literature are given as follows:**

100

- 101 • In this study, we divided an inspired by the encoder layer of the U-shaped segmentation  
102 algorithm and connected the model we designed to the fully connected layer. Therefore, we  
103 have fused the Generalised Dice Loss(GDL) function used in multi-class segmentation with  
104 the Focal Loss(FL) function in such a network.
- 105 • Non-Local Means and Estimate sigma algorithms are first fused to eliminate noise in MR  
106 images by us.
- 107 • Contrast Limited Adaptive Histogram Equalization (CLAHE) algorithm used for histogram  
108 equalization to enhance MR images.
- 109 • A fully connected Deep Convolutional neural network with Residual blocks is proposed to  
110 classify AD.
- 111 • A fusion loss function increased the network's test accuracy in classifying AD from MR  
112 images.

113

114 The second section, consisting of the material and method section, gives detailed information about  
115 the pre-processing stages of the data set and the proposed model. The practical applications of the model  
116 and the test results obtained from the proposed model are evaluated and discussed in the 3rd chapter, the  
117 discussion section. Finally, the work done in the 4th chapter is summarized, and suggestions for future  
118 studies are shared.

119

## 120 **Materials & Methods**

### 121 **MRI dataset**

122

123 The KAGGLE online community obtained the dataset [Dubey, 2023]. The dataset obtained from  
124 KAGGLE consists of 5121 axial images collected from different websites. The images in the  
125 dataset were collected and labeled into four different classes. These are no dementia, very mild  
126 dementia, mild dementia, and moderate dementia. There is no information about the age of the  
127 patients in the MR images obtained from the patients. The training dataset consists of MR images  
128 of 2560 healthy (ND), 1792 very mild dementia (vmD), 717 mild dementia (miD), and 52  
129 moderate dementia (mD) individuals. The test dataset consists of MR images of 640 healthy (NC),  
130 448 very mild dementia (vmD), 179 mild dementia (miD), and 12 moderate dementia (mD)  
131 individuals. The resolution of the images is 176x208. Samples are shown in Fig. 1. No other  
132 circumstances of the MR images obtained were specified.

133

134

135 **Fig. 1.** Samples of axial images in the Kaggle data set

136

### 137 **Dataset Pre-processing**

138 Various image restoration techniques are used in the Kaggle AD dataset to increase the model's  
139 training and test accuracy. First, the Non-Local Means (NLM) algorithm was applied to the  
140 images. Then, the image noise was de-noised using the weighted average of the pixel  
141 neighborhoods with similarity. Also, to improve performance when calculating the similarity of  
142 each pixel, instead of considering just one pixel, a small area of pixels is chosen around it, given  
143 by the `small_window` parameter. `Patch_Size=2` and `Patch_Distance=1` was selected to increase  
144 the noise removal performance of the NLM algorithm. Finally, `Estimate_sigma` is fused with the  
145 NLM algorithm to improve the performance of the proposed model.

146 The resulting images were passed through the CLAHE algorithm. Contrast-limited histogram  
147 equalization is performed by dividing images into small blocks called tiles in CLAHE in the  
148 OpenCV library. As a result of the experimental studies, the clipping level in CLAHE was chosen  
149 as 2.6. Samples of 4 different classes are shown in Fig. 2., showing the MR images in the Kaggle  
150 dataset before and after the noise removal and CLAHE. In Fig. 2., the pictures in the top line are  
151 the MR images before the image pre-processing techniques, and the images in the bottom line are  
152 the MR images obtained after the image pre-processing methods. The pre-processed training data  
153 set was doubled by applying random shifting, random rotation, random rescaling, and random  
154 horizontal and vertical flip methods.

155

156 **Fig. 2.** Samples of image pre-processing techniques in the Kaggle data set: the pictures in the top  
157 line are the MR images before the image pre-processing techniques, and the images in the bottom  
158 line are the MR images obtained after the pre-processing image methods.

159

### 160 **The Proposed Categorical Generalized Focal Dice Loss Function**

161 The proposed Hybrid Loss function is a fused model of the Generalized Dice Loss (GDL) and  
162 Focal Loss (FL) [Sudre et al., 2017; Lin et al., 2022]. The FL function formula is shown in Eq. 1.

163

$$164 \quad FL = -\alpha_t(1 - p_t)^\gamma \log(p_t) \quad (1)$$

165

166 As seen in Eq. 1., Contrary to Cross-entropy (CE), Loss of Focus prevents suppression of CE Loss  
167 in large class imbalances. Thus, the Negatives that make up most of the Loss are reduced. Adding  
168  $\alpha$  to Focal Loss in Balanced Cross Entropy balances positive and negative samples. In addition,  
169 the adjustable focusing parameter  $\gamma \geq 0$  and the cross-entropy Loss modulating factor  $(1 - p_t)$  was  
170 added to reduce the weight of easy-to-learn samples and to enable the deep-learning model to focus  
171 on difficult-to-train samples. As a result of the experimental studies performed in this study, we  
172 chose  $\gamma=2$  and  $\alpha=4$ , where  $p$  is the model's predicted probability for the class [Lin et al., 2022].

173 The most significant disadvantage of Dice Loss is that although it has a good training score, its  
174 test score is low due to its poor response to class imbalances. As a solution to this, Sudre et al.  
175 transformed the Generalized Dice Score (GDS) function proposed by Crum et al. to score multi-

176 class segmentation into a loss function named Generalized Dice Loss(GDL) [Crum et al., 2006].  
 177 The GDL function formula is shown in Eq. 2.

178

$$179 \quad GDL = 1 - 2 \frac{\sum_{l=1}^2 w_l \sum_n r_{ln} p_{ln} + \epsilon}{\sum_{l=1}^2 w_l \sum_n r_{ln} + p_{ln} + \epsilon} \quad (2)$$

180

181

182 Where  $r_l$  is the ground truth, and  $p_l$  is the predicted value.  $\epsilon$  is a smoothing value for fine-tuning.

183 Here  $w_l$  is used to provide immutability to different labeled sets where  $w_l$  is formulated as shown

184 in E.q. 3.

$$185 \quad w_l = \frac{1}{(\sum_{n=1} r_{ln})^2} \quad (3)$$

186

187 Where  $r_l$  is the ground truth. In this study, FL and GD, seen as robust models in multi-class  
 188 segmentation, were fused to predict four different classes of AD, as shown in E.q. 4.

189

$$190 \quad \text{Fusion\_Loss} = (1 - \text{lamda}) * \text{GDL} + \text{lamda} * \text{FL} \quad (4)$$

191

192 The lambda value was chosen as 0.5 because of experimental studies.

193

### 194 **Performance Metrics**

195 Accuracy, Sensitivity, and Specificity metrics were used to measure the performance of the  
 196 proposed deep learning-based classification model. Accuracy is the ratio of correctly predicted  
 197 samples to the sum of all correct and incorrectly guessed samples; Sensitivity, or recall, is the ratio  
 198 of positively correctly predicted samples to the sum of negative incorrectly predicted samples and  
 199 correctly predicted positive samples. Specificity (Spec) represents the ratio of correctly predicted  
 200 negative samples to the sum of correctly predicted negative samples and incorrectly predicted  
 201 positive samples.

202

203

204

205

### 206 **The Proposed Methodology**

207 The end-to-end automatically AD classifier block diagram is shown in Fig. 3. The section  
208 including CLAHE covers the pre-processing stage of the dataset, and the section after CLAHE  
209 covers the training and testing of the model.

210

211

212 **Fig. 3** End-to-end automatically DCNN-based AD classifier block diagram

213

### 214 **The Proposed Deep Learning Model**

215 In the proposed deep learning architecture, 2xConvolutional2D blocks with 3x3 filters are used in  
216 all layers before the fully connected layer. In addition, the Xavier was used as the weight initializer  
217 function [Glorot et al., 2010]. Group Normalization (GN) is the normalizer, and ReLU is the  
218 activation function of the proposed model [Wu and He, 2020]. Wu and He demonstrated with  
219 various experiments how superior the group normalization technique is to other normalization  
220 methods.

221 Besides, ADAM was used as the optimizer to optimize the weights of the proposed model [Kingma  
222 et al., 2015]. In the last layer, Softmax was used as an activation function to find out which class  
223 the MR image belongs to the AD class. If we pay attention to the proposed model, it is seen that  
224 the U-shaped network is formed by taking the deconvolution part and adding the Fully connected  
225 network. Deep Neural networks are profound networks due to the multitude of layers. Therefore,  
226 the information learned in the first layers can be forgotten. The residual blocks(ResNet Block)  
227 ensure that the convolutional layers do not forget the information they learned in the first layers of  
228 the network. In the proposed model, Residual blocks are followed by 2×2 maximum pooling(Max-  
229 pool), in which the feature maps' spatial dimensions (height and width) are reduced by half. Max-  
230 pool reduces the computational cost by reducing the number of trainable parameters. The layers  
231 of the proposed deep learning architecture are shown in Fig. 4. in detail.

232

233

234

**Fig. 4.** Detailed representation of the proposed architecture

235

236

237

**238 Proposed Model's Experimental Studies**

239 This section explains the experimental studies of the proposed deep learning architecture on the  
240 KAGGLE dataset in detail.

241

**242 Employed hardware materials**

243 Experimental studies of the proposed architecture were conducted with a computer equipped with  
244 Intel(R) Core(TM) i5-8300H @ 2.30 GHz CPU, 32 GB RAM, and NVIDIA GTX1050 4 GB GPU.

245 In addition, the deep learning ecosystem consists of artificial intelligence libraries with Python 3.7  
246 programming language based on Anaconda. Libraries and ecosystems are entirely open source.

247 The dataset consists of training, validation, and test datasets. 20% of the training dataset was used  
248 as a validation dataset using the scikit-learn library. We performed 5-fold cross-validation to  
249 measure the training dataset's heterogeneity and the model's fit.

250

**251 Comparison of parameters**

252 The model used in the proposed study and the models used in the other literature were analyzed  
253 comparatively regarding the number of parameters. As can be seen from the comparisons in Table  
254 1, the proposed model is the one with the smallest parameter. It can be seen from Table 1 that the  
255 model with the smallest parameter is the recommended model.

256

257 **Table1.** Comparison of parameters and their computational efficiency

258

**259 Comparison of loss functions**

260 The proposed fusion loss function has been analyzed in comparison with the most used Mean  
261 Absolute Error (MAE), Root Mean Squared Error (RMSE), Cross-Entropy, FL, and GDL loss  
262 function for classification in the literature. As can be seen from Table 2, the proposed fusion loss  
263 function is the most suitable loss function for the proposed architecture.

264

265 **Table2.** Effects of different loss functions on the proposed architecture.

266

267

268

**269 Settings and studies on the KAGGLE dataset**

270 Using our deep learning architecture, we performed binary classification, i.e., distinguishing NC  
271 and AD, and multi-class classification (NC, very mild AD, mild AD, moderate AD) experimental  
272 studies on the KAGGLE dataset. The deep learning network was trained for 15 thousand epochs  
273 for these two studies. After 15.000 epochs, the validation accuracy of the network remained  
274 constant at around 0.99. The minibatch size is 32, and ADAM is chosen as the optimizer.  
275 Numerical information about the data set used in training the proposed model is listed in Table 3.  
276 As can be seen from Table 3, there is a significant imbalance between classes. In this case, the  
277 benefits of data augmentation methods will be limited. Therefore, GDL and FL, which are  
278 successful and robust loss functions in class imbalances, are proposed as a solution to the class  
279 imbalance of the data set.

280

281 **Table 3.** Slice-based MR image counts used for train, validation, and testing of the KAGGLE  
282 Data set on which the proposed model is trained and tested.

283

284

**285 Experimental results and analysis**

286 In this section, experimental results are shared, and comparative analyzes are made with other  
287 studies in the literature. In addition, information is given about the deep learning models used for  
288 detecting AD and how they train the dataset on the performance criteria they use. A slice-based  
289 data set was used in this study. The Kaggle dataset is a low-resolution and slice-based dataset  
290 collected on different websites. In addition, class imbalances are also very high in the dataset.  
291 Also, the Kaggle dataset's having axial views is another challenge. For these reasons, the Kaggle  
292 dataset is very challenging. The most significant difficulty of all the literature and proposed  
293 research studies is distinguishing AD from NC in the MCI stage. If AD is successfully detected in  
294 the MCI stage, the effects of this neurodegenerative and irreversible disease can be slowed down.  
295 In addition, one of the most critical challenges is to detect NCs (very MCI) that may have AD.  
296 This study focused on two different experimental studies: i) distinguishing NC from AD at the  
297 MCI stage; ii) To successfully classifying MR images with NC, vMCI, MCI, and MC. For this

298 reason, articles in the literature that made these two different experimental studies and analyzed  
299 their results were examined. Validation Accuracy and Validation Loss values obtained using the  
300 Categorical Generalized focal Membrane loss function of the proposed model are shown  
301 graphically in Figure 5 and Figure 6.

302

303

304 **Fig. 5.** ResBlock Fully Connected CNN Validation Loss and Validation Accuracy Results

305

306

307 **Fig. 6.** ResBlock Fully Connected CNN Validation Loss and Validation Accuracy Results

308

309 The comparative performance results of our proposed fusion loss-based deep learning architecture  
310 are shown in Table 4 and Table 5. The proposed deep learning architecture achieved accuracy  
311 values of 0.973 in binary classification and 0.982 in multi-class classification. At the same time, it  
312 obtained high sensitivity and specificity values compared to other studies in the literature.

313

314 **Table 4.** Experimental results for NC and AD binary classification

315

316 **Table 5.** Experimental results for multi-class classification (NC, vmiD, miD, mD)

317

## 318 **Discussion**

319 This study proposes a deep learning-based model with fusion loss for diagnosing and classifying  
320 AD. The Kaggle dataset, the most challenging AD dataset, was used to compare the proposed  
321 architecture with other studies in the literature. High accuracy values of up to 0.99 were obtained  
322 in other publicly available datasets (OASIS and ADNI) used in the literature. The Kaggle dataset  
323 has four classes: vmiD, miD, mD, and NC. The proposed fusion loss deep learning model showed  
324 a higher performance than other studies in the literature. In addition, Ensemble-based deep learning  
325 algorithms are generally emphasized in the literature. The deep learning architecture proposed in  
326 this paper also dramatically reduces computation. However, the minibatch could not be increased  
327 enough due to hardware limitations. In addition, resizing was not done because the resolution of  
328 the data line was low. Therefore, the number of epochs determined for training the proposed model

329 may be higher than those used by other models. However, the parameter number of the proposed  
330 architecture is considerably smaller than the parameter numbers of different architectures in the  
331 literature.

332

### 333 **Conclusions**

334 This study proposes a fusion loss deep learning model using the group normalization technique  
335 with residual blocks to detect three different classes (vmiD, miD, mD) of AD disease. The  
336 proposed model is trained on the KAGGLE dataset, a very challenging dataset that includes three  
337 other dementia classes (vmiD, miD, mD) and normal cognitive status. We tried to solve the large  
338 class imbalance in the Kaggle dataset using the Categorical Generalised Focal Dice Loss function  
339 proposed in this study. In the proposed model, FL and GDL loss functions are used successfully  
340 in multi-class segmentation by fusing them. FL and GDL were used separately in the proposed  
341 model, and 84% to 88% accuracy was achieved, while an accuracy value of 0.982 was obtained in  
342 the model with the fused loss function. Compared to the latest technology studies in the literature,  
343 the proposed model has achieved very high success in binary classification (NC and AD) and  
344 multi-class classification (vmiD, miD, mD, NC). Although the proposed architecture showed high  
345 performance on a challenging dataset, it must be tested on an MR device in real-time.

346

### 347 **Acknowledgements**

348 The authors extend their appreciation to the Deputyship for Research & Innovation, Ministry of  
349 Education in Saudi Arabia for funding this research work through project number (IF-PSAU-  
350 2021/01/18563).

351

### 352 **Ethical approval**

353 This article does not contain any data, or other information from studies or experimentation, with  
354 the involvement of human or animal subjects.

355

### 356 **Conflicts of interest**

357 The authors declare that there is no conflict to interest related to this paper.

358

### 359 **Raw Data Availability**

360

361 Dubey, S. Alzheimer's dataset (4 class of images) [online] Available:  
362 <https://www.kaggle.com/datasets/tourist55/alzheimers-dataset-4-class-of-images> (Accessed 17  
363 July 2023).

364

365 **Source code is available at GitHub:**366 <https://github.com/kpolat14/data-weighting-model-and-classification>

367

368 **References**

369

370 Alzheimer's disease facts and figures. *Alzheimer's Dement.*, 18: 700-789,  
371 2022. <https://doi.org/10.1002/alz.12638>.

372 Alberdi, A., Weakley, A., Schmitter-Edgecombe, M., Cook, D.J., Aztiria, A., Basarab, A.,  
373 Barrenechea, M.(2018) Smart home-based prediction of multidomain symptoms related to  
374 Alzheimer's disease. *IEEE J. Biomed. Health Inform.* 2018;22:1720–31.

375 Alorf, A., Khan, M.U.G.(2022) Multi-label classification of Alzheimer's disease stages from  
376 resting-state fMRI-based correlation connectivity data and deep learning. *Comput Biol*  
377 *Med.* 2022 Dec;151(Pt A):106240. doi: 10.1016/j.combiomed.2022.106240. Epub 2022  
378 Nov 9. PMID: 36423532.

379 Armstrong, N., Nugent, C., Moore, G., Finlay, D.(2009) In *International conference on smart*  
380 *homes and health telematics*; Springer, pp 25-31.

381 Babalola, K.O., Patenaude, B., Aljabar, P., Schnabel, J., Kennedy, D., Crum, W., Smith, S.,  
382 Cootes, T., Jenkinson, M., Rueckert, D.(2009). Anevaluationoffour automatic methods of  
383 segmenting the subcortical structures in the brain. *Neuroimage* 2009;47(4): 1435–47.

384 Ba, J., Kingma, DP, , 2015. Adam: a method for stochastic optimization. in: *International*  
385 *Conference on Learning Representations (ICLR)*, pp.1–11.

386 Chandra, A., Dervenoulas, G., Politis, M.(2019). Magnetic resonance imaging in Alzheimer's  
387 disease and mild cognitive impairment. *J. Neurol.* 2019;266:1293–302.

388 Coppola, J.F., Kowtko, M.A., Yamagata, C., Joyce, S.(2013). Applying mobile application  
389 development to help dementia and Alzheimer patients. *Wilson Center Soc. Entrepreneur.*  
390 2013;16. Paper.

391 Crum, W., Camara, O., Hill, D.: Generalized Overlap Measures for Evaluation and Validation in  
392 *Medical Image Analysis*. *IEEE TMI* 25(11), 1451 {1461 (nov 2006)

393 Dubey, S. Alzheimer's dataset (4 class of images) [online] Available: [https://www.](https://www.kaggle.com/datasets/tourist55/alzheimers-dataset-4-class-of-images)  
394 [kaggle.com/datasets/tourist55/alzheimers-dataset-4-class-of-images](https://www.kaggle.com/datasets/tourist55/alzheimers-dataset-4-class-of-images). (Accessed 07 Feb  
395 2023).

- 396 Frizzell, T.O., Glashutter, M., Liu, C.C., Zeng, A., Pan, D., Hajra, S.G., D'Arcy, R.C.N., Song  
397 X.(2022). Artificial intelligence in brain MRI analysis of Alzheimer's disease over the  
398 past 12 years: A systematic review. *Ageing Res Rev.* 2022 May;77:101614. doi:  
399 10.1016/j.arr.2022.101614. Epub 2022 Mar 28. PMID: 35358720.
- 400 Glorot, X., Bengio, Y, 2010. Understanding the difficulty of training deep feedforward neural  
401 networks. In *Aistats*, volume 9, pages 249–256.
- 402 Gopinadhan, A., Angeline Prasanna, G., Anbarasu, S.(2022). AD-EHS: Alzheimer's disease  
403 severity detection using efficient hybrid image segmentation, *Advances in Engineering*  
404 *Software*, Volume 173, 2022, 103234, ISSN 0965-9978,  
405 <https://doi.org/10.1016/j.advengsoft.2022.103234>.
- 406 Jung, E., Luna, M., Park, S.H.(2023). Conditional GAN with 3D discriminator for MRI generation  
407 of Alzheimer's disease progression. *Pattern Recognition*, Volume 133, 2023,109061,  
408 ISSN 0031-3203, <https://doi.org/10.1016/j.patcog.2022.109061>.
- 409 Lahmiri, S.(2023). Integrating convolutional neural networks, kNN, and Bayesian optimization  
410 for efficient diagnosis of Alzheimer's disease in magnetic resonance images.  
411 *Biomedical Signal Processing and Control*, Volume 80, Part 2, 2023, 104375, ISSN  
412 1746-8094, <https://doi.org/10.1016/j.bspc.2022.104375>.
- 413 Lin, T.Y., Goyal, P., Girshick, R., He K., Dollár, P.(2020). Focal Loss for Dense Object Detection.  
414 in *IEEE Transactions on Pattern Analysis and Machine Intelligence*, vol. 42, no. 2, pp.  
415 318-327, 1 Feb. 2020, doi: 10.1109/TPAMI.2018.2858826.
- 416 Loddo, A., Buttau, S., Di Ruberto, C.(2021) Deep learning based pipelines for Alzheimer's disease  
417 diagnosis: A comparative study and a novel deep-ensemble method. *Comput Biol Med.*  
418 2022 Feb;141:105032. doi: 10.1016/j.compbio.2021.105032. Epub 2021 Nov 21.  
419 PMID: 34838263.
- 420 Mehmood, A., Yang, S., Feng, Z., Wang, M., Ahmad, A.S., Khan, R., Maqsood, M., Yaqub,  
421 M.(2021). A Transfer Learning Approach for Early Diagnosis of Alzheimer's Disease  
422 on MRI Images. *Neuroscience*, Volume 460, 2021, Pages 43-52.
- 423 Raghavaiah, P., Varadarajan, S.(2021) Novel deep learning convolution technique for recognition  
424 of Alzheimer's disease, *Materials Today: Proceedings*, Volume 46, Part 9, 2021, Pages  
425 4095-4098, ISSN 2214-7853, <https://doi.org/10.1016/j.matpr.2021.02.626>.

- 426 Sathish Kumar, L., Hariharasitaraman, S., Narayanasamy, K., Thinakaran, K., Mahalakshmi, J.,  
427 Pandimurugan. V.(2022). AlexNet approach for early stage Alzheimer's disease  
428 detection from MRI brain images. *Materials Today: Proceedings*, Volume 51, Part 1,  
429 2022, Pages 58-65, ISSN 2214-7853, <https://doi.org/10.1016/j.matpr.2021.04.415>.
- 430 Sharma, S., Guleria, K., Tiwari, S., Kumar, S.(2022). A deep learning based convolutional neural  
431 network model with VGG16 feature extractor for the detection of Alzheimer Disease  
432 using MRI scans, *Measurement: Sensors*, Volume 24, 2022, 100506, ISSN 2665-  
433 9174, <https://doi.org/10.1016/j.measen.2022.100506>.
- 434 Shanmugam, J.V., Duraisamy, B., Simon, B.C., Bhaskaran, P.(2022). Alzheimer's disease  
435 classification using pre-trained deep networks. *Biomedical Signal Processing and*  
436 *Control*, Volume 71, Part B, 2022, 103217, ISSN 1746-8094,  
437 <https://doi.org/10.1016/j.bspc.2021.103217>.
- 438 Sudre, C.H., Li, W., Vercauteren, T., Ourselin, S., Jorge Cardoso, M. (2017). Generalised Dice  
439 Overlap as a Deep Learning Loss Function for Highly Unbalanced Segmentations. In:  
440 , et al. *Deep Learning in Medical Image Analysis and Multimodal Learning for Clinical*  
441 *Decision Support . DLMIA ML-CDS 2017 2017. Lecture Notes in Computer Science()*,  
442 vol 10553. Springer, Cham. [https://doi.org/10.1007/978-3-319-67558-9\\_28](https://doi.org/10.1007/978-3-319-67558-9_28).
- 443 Wu, Y., He, K. Group Normalization. *Int J Comput Vis* 128, 742–755 (2020).  
444 <https://doi.org/10.1007/s11263-019-01198-w>

**Table 1** (on next page)

Comparison of parameters and their computational efficiency

Comparison of parameters and their computational efficiency

1 **Table1.** Comparison of parameters and their computational efficiency

<b>Architectures</b>	<b>Parameter(M)</b>
VGG16[Sharma et al.]	134.27
Alexnet[Loddo et al.]	62.38
Resnet 101[Loddo et al.]	44.5
Inception ResNetv2[Loddo et al.]	54.5
Proposed Architecture	5.45

2

3

**Table 2** (on next page)

Effects of different loss functions on the proposed architecture.

Effects of different loss functions on the proposed architecture.

1 **Table2.** Effects of different loss functions on the proposed architecture.

<b>Methods</b>	<b>Performance metrics</b>		
	<b>Accu</b>	<b>Sens</b>	<b>Spec</b>
Cross-entropy	0.966	0.966	0.982
MAE[Loddo et al.]	0.932	0.932	0.934
RMS[Loddo et al.]	0.956	0.959	0.957
FL[Loddo et al.]	0.927	0.930	0.928
GDL	0.965	0.968	0.966
<b>Our Fusion Loss</b>	<b>0.982</b>	<b>0.982</b>	<b>0.989</b>

2

**Table 3**(on next page)

Slice-based MR image counts used for train, validation, and testing of the KAGGLE Data set on which the proposed model is trained and tested.

Slice-based MR image counts used for train, validation, and testing of the KAGGLE Data set on which the proposed model is trained and tested.

1 **Table 3.** Slice-based MR image counts used for train, validation, and testing of the KAGGLE  
2 Data set on which the proposed model is trained and tested.

3

<b>Data set name</b>	<b>NC</b>	<b>vmiD</b>	<b>miD</b>	<b>mD</b>
Training data set	2050	1075	573	42
Train+Data Augmented	7170	4659	2007	146
Validation data set	510	717	287	10
Test data set	640	448	179	12

4

5

**Table 4**(on next page)

Experimental results for NC and AD binary classification

Experimental results for NC and AD binary classification

1 **Table 4.** Experimental results for NC and AD binary classification

<b>Methods</b>	<b>Performance metrics</b>		
	<b>Accu</b>	<b>Sens</b>	<b>Spec</b>
Deep-Ensemble[Loddo et al.]	0.966	0.966	0.982
AlexNet[Loddo et al.]	0.897	0.898	0.897
ResNet-101[Loddo et al.]	0.961	0.961	0.961
Inception-ResNet-v2[Loddo et al.]	0.912	0.914	0.912
<b>(Our Methodology)</b>	<b>0.973</b>	<b>0.975</b>	<b>0.988</b>

2

3

**Table 5** (on next page)

Experimental results for multi-class classification (NC, vmiD, miD, mD)

Experimental results for multi-class classification (NC, vmiD, miD, mD)

1 **Table 5.** Experimental results for multi-class classification(NC, vmiD, miD, mD)

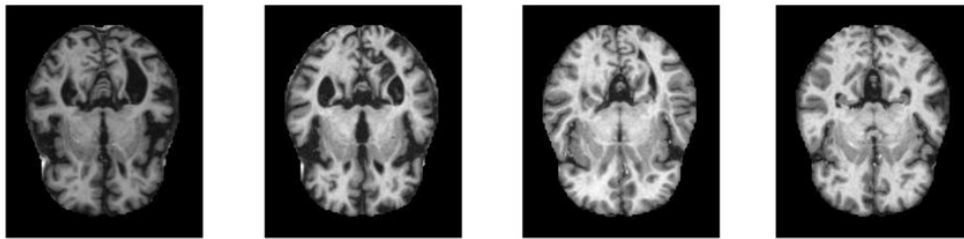
<b>Methods</b>	<b>Performance metrics</b>		
	<b>Accu</b>	<b>Sens</b>	<b>Spec</b>
Deep-Ensemble[Loddo et al.]	0.971	0.967	0.982
Neural Nets with VGG16 [Sharma et al.,]	0.904	0.905	0.904
AlexNet[Loddo et al.]	0.893	0.906	0.817
ResNet-101[Loddo et al.]	0.965	0.978	0.961
Inception-ResNet-v2[Loddo et al.]	0.897	0.901	0.856
<b>(Our Methodology)</b>	<b>0.982</b>	<b>0.982</b>	<b>0.989</b>

2

# Figure 1

Samples of axial images in the Kaggle data set

Samples of axial images in the Kaggle data set



(a) No dementia    (b) Very mild dementia    (c) Mild dementia    (d) Moderate dementia

**Fig. 1.** Samples of axial images in the Kaggle data set

## Figure 2

Samples of image pre-processing techniques in the Kaggle data set

Samples of image pre-processing techniques in the Kaggle data set

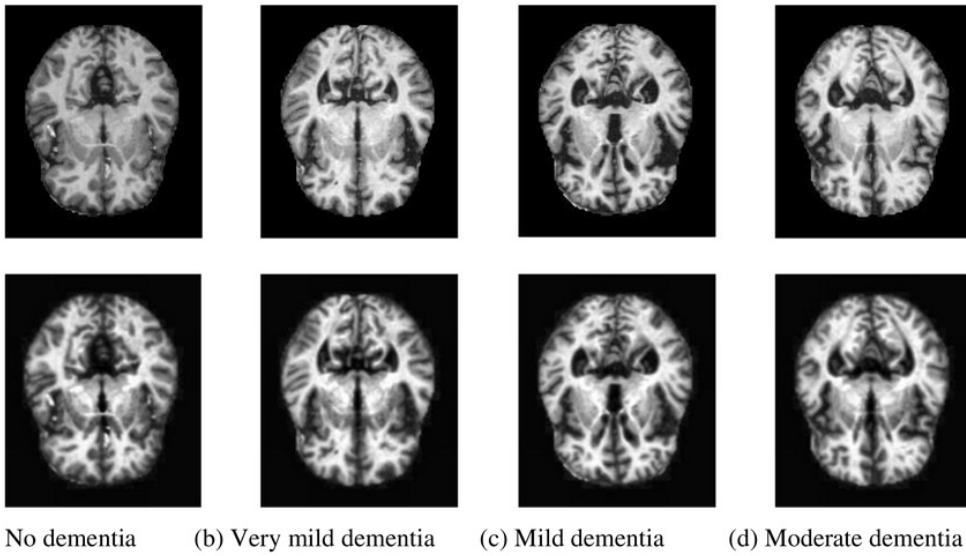


**Fig. 2.** Samples of image pre-processing techniques in the Kaggle data set: the pictures in the top line are the MR images before the image pre-processing techniques, and the images in the bottom line are the MR images obtained after the pre-processing image methods.

## Figure 3

End-to-end automatically DCNN-based AD classifier block diagram

End-to-end automatically DCNN-based AD classifier block diagram

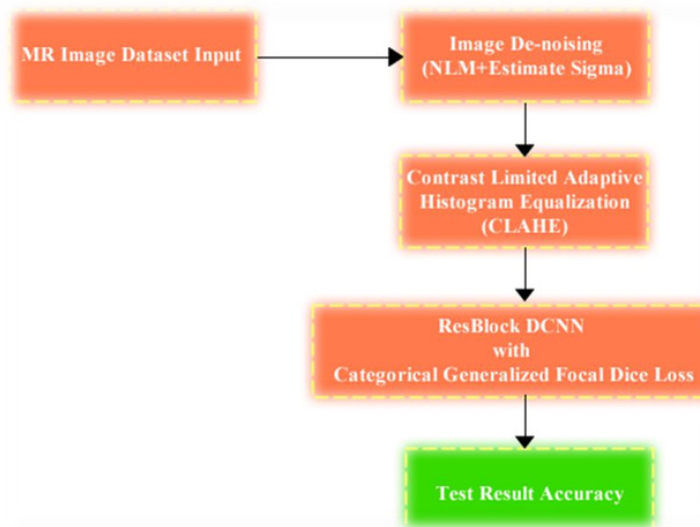


**Fig. 3** End-to-end automatically DCNN-based AD classifier block diagram

## Figure 4

Detailed representation of the proposed architecture

Detailed representation of the proposed architecture

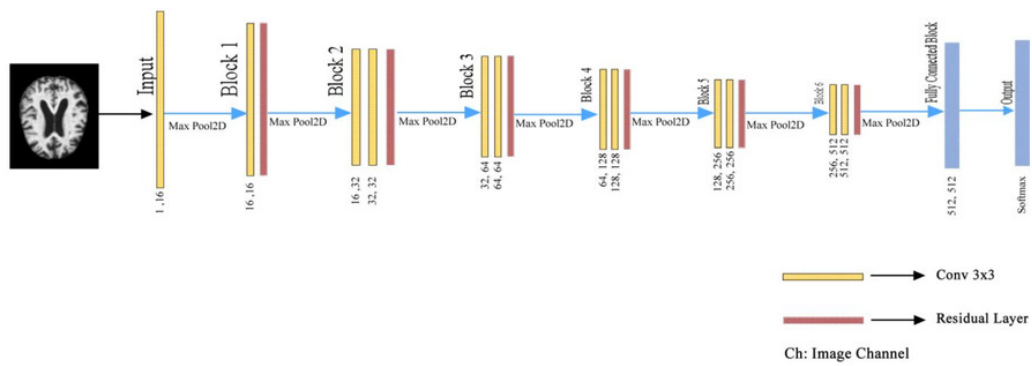


**Fig. 4.** Detailed representation of the proposed architecture

## Figure 5

ResBlock Fully Connected CNN Validation Loss and Validation Accuracy Results

ResBlock Fully Connected CNN Validation Loss and Validation Accuracy Results

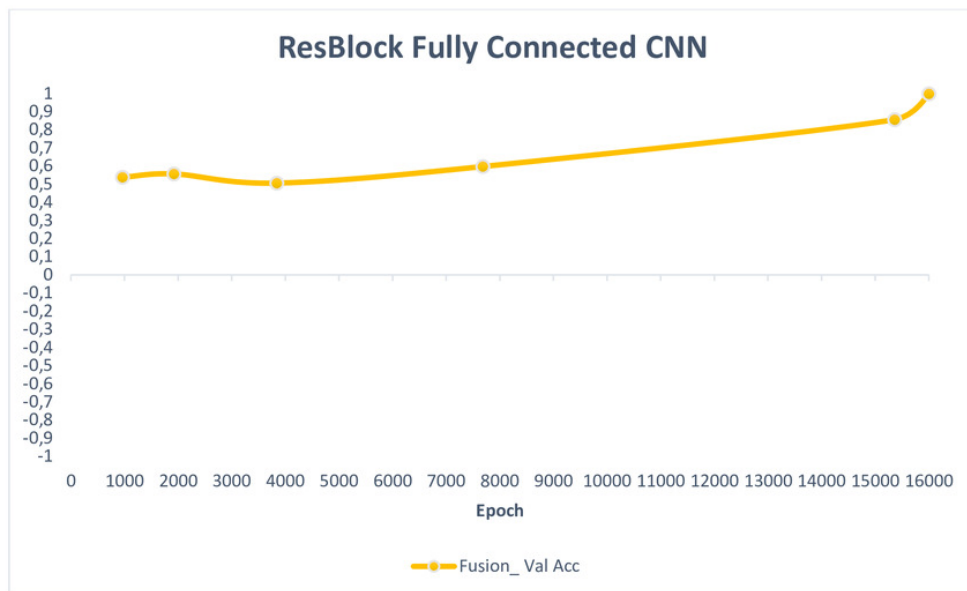
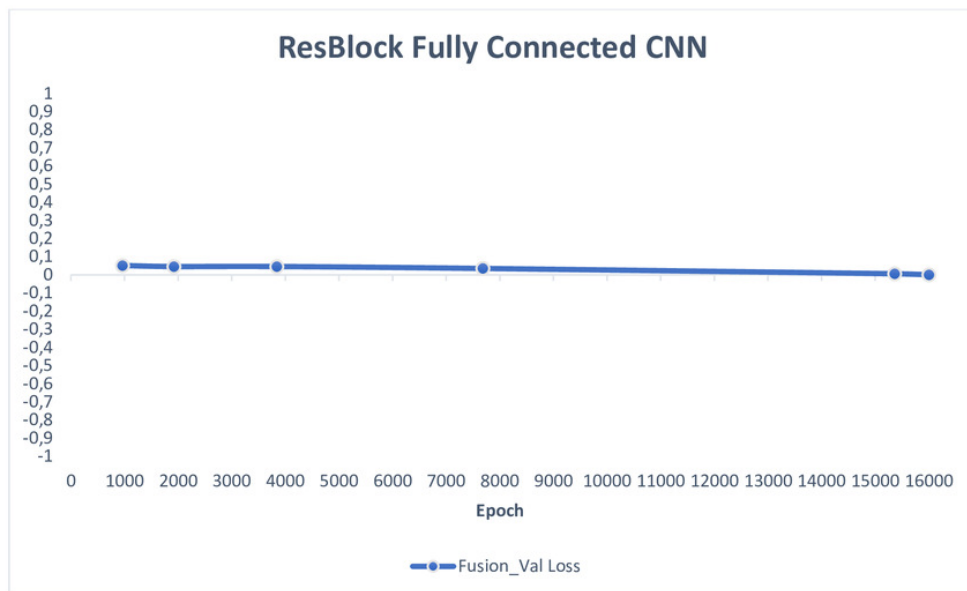


Fig. 5. ResBlock Fully Connected CNN Validation Loss and Validation Accuracy Results

## Figure 6

ResBlock Fully Connected CNN Validation Loss and Validation Accuracy Results

ResBlock Fully Connected CNN Validation Loss and Validation Accuracy Results



**Fig. 6.** ResBlock Fully Connected CNN Validation Loss and Validation Accuracy Results